2005

Rapid and Reversible Generation of a Microscale pH Gradient Using Surface Electric Fields

Eric L. May
Iowa State University

Andrew C. Hillier
Iowa State University, hillier@iastate.edu

Rapid and Reversible Generation of a Microscale pH Gradient Using Surface Electric Fields

Abstract

We report a method for the rapid and reversible generation of microscale pH gradients using a spatially varied electric field. A linear gradient in electrochemical potential is produced on an electrode surface consisting of a platinum catalyst layer on indium–tin oxide-coated glass by the application of two different potential values at spatially distinct surface locations. The resulting potential gradient drives the oxidation and reduction of water at different rates along the surface, as dictated by the local applied potential. A nonuniform distribution of pH in the neighboring solution results due to the variation in surface reaction rates. The extent and magnitude of the pH gradient can be controlled by the appropriate selection of applied potential values. In addition, the gradient can be rapidly turned on or off and reversibly switched between various profiles. The size of the pH gradient can be readily modified by changing the dimensions of the electrode and contact pads to allow integration into chip-scale devices. Characteristics of the pH gradient are described, including experimental and theoretical evidence of significant improvement in time response over competing methods for the generation of microscale pH gradients.

Disciplines

Chemical Engineering | Chemistry

Comments

This article is from *Analytical Chemistry*77 (2005): 6487-6493, doi:10.1021/ac051014w. Posted with permission.

Anal. Chem. **2005,** *77,* 6487−6493

Technical Notes

Rapid and Reversible Generation of a Microscale pH Gradient Using Surface Electric Fields

Erin L. May and Andrew C. Hillier*

Department of Chemical Engineering and Department of Chemistry, Iowa State University, Ames, Iowa 50011

We report a method for the rapid and reversible generation of microscale pH gradients using a spatially varied electric field. A linear gradient in electrochemical potential is produced on an electrode surface consisting of a platinum catalyst layer on indium−tin oxide-coated glass by the application of two different potential values at spatially distinct surface locations. The resulting potential gradient drives the oxidation and reduction of water at different rates along the surface, as dictated by the local applied potential. A nonuniform distribution of pH in the neighboring solution results due to the variation in surface reaction rates. The extent and magnitude of the pH gradient can be controlled by the appropriate selection of applied potential values. In addition, the gradient can be rapidly turned on or off and reversibly switched between various profiles. The size of the pH gradient can be readily modified by changing the dimensions of the electrode and contact pads to allow integration into chip-scale devices. Characteristics of the pH gradient are described, including experimental and theoretical evidence of significant improvement in time response over competing methods for the generation of microscale pH gradients.

Lab on a chip concepts for microfabricated analytical devices consisting of various functions and sample preparation capabilities on a miniaturized scale have become increasingly popular due to portability, disposability, and on-demand processing capabilities.[1−3] For analytical techniques, the reduction in size can significantly reduce sample consumption, decrease the time required to isolate a compound,[4] and be more conducive to parallel processing, providing the capability for high-throughput analysis.[5]

A variety of miniaturized devices and components have been demonstrated. Examples include a variety of macroscale devices fabricated in the microscale, such as pumps, valves, sensors, power supplies, and fluidic processes.[6−9] Furthermore, a variety of analytical methods have been reduced to practice on the microscale, including gas chromatography,[10] liquid chromatography,[11,12] flow cytometry,[13,14] and mass spectrometry.[15−17] Improved performance for chip-based analytics include electrophoresis[18−20] devices that can separate nucleic acids in less than 1 min[21] and perform more complicated tasks such as DNA sequencing in less than 20 min.[22]

Miniaturizing analytical devices involves solving a variety of challenges. Simple tasks such as sample injection and flow control require new technologies at the microscale. The challenges increase for more complicated processes involving mixing, reaction, and detection at the microscale. Electrophoresis represents a relatively straightforward process to miniaturize. However, performing isoelectric focusing on the microscale is considerably more complex. The requisite pH gradient combined with the applied electric field needed to isolate compounds by charge must be generated and placed with spatial control within a microscale platform. At the macroscale, pH gradients are generated from the

* To whom correspondence should be addressed. E-mail: hillier@iastate.edu.

(1) Landers, J. P. *Anal. Chem.* **2003**, *75*, 2919−2927.
(2) Auroux, P. A.; Iossifidis, D.; Reyes, D. R.; Manz, A. *Anal. Chem.* **2002**, *74*, 2637−2652.
(3) Verpoorte, E. *Electrophoresis* **2002**, *23*, 677−712.
(4) Ueda, M.; Kiba, Y.; Abe, H.; Arai, A.; Nakanishi, H.; Baba, Y. *Electrophoresis* **2000**, *21*, 176−180.
(5) Liu, S. R.; Elkin, C.; Kapur, H. *Electrophoresis* **2003**, *24*, 3762−3768.
(6) Hartshorne, H.; Backhouse, C. J.; Lee, W. E. *Sens. Actuators, B* **2004**, *99*, 592−600.
(7) Wang, J. *Anal. Chim. Acta* **2004**, *507*, 3−10.
(8) Collins, G. E.; Wu, P.; Lu, Q.; Ramsey, J. D.; Bromund, R. H. *Lab Chip* **2004**, *4*, 408−411.
(9) Stone, H. A.; Stroock, A. D.; Ajdari, A. *Annu. Rev. Fluid Mech.* **2004**, *36*, 381−411.
(10) Shortt, B. J.; Darrach, M. R.; Holland, P. M.; Chutjian, A. *J. Mass Spectrom.* **2005**, *40*, 36−42.
(11) Davis, M. T.; Lee, T. D. *J. Am. Soc. Mass Spectrom.* **1998**, *9*, 194−201.
(12) Pergantis, S. A.; Heithmar, E. M.; Hinners, T. A. *Anal. Chem.* **1995**, *67*, 4530−4535.
(13) Chun, H. G.; Chung, T. D.; Kim, H. C. *Anal. Chem.* **2005**, *77*, 2490−2495.
(14) McClain, M. A.; Culbertson, C. T.; Jacobson, S. C.; Ramsey, J. M. *Anal. Chem.* **2001**, *73*, 5334−5338.
(15) Badman, E. R.; Cooks, R. G. *J. Mass Spectrom.* **2000**, *35*, 659−671.
(16) Riter, L. S.; Peng, Y. A.; Noll, R. J.; Patterson, G. E.; Aggerholm, T.; Cooks, R. G. *Anal. Chem.* **2002**, *74*, 6154−6162.
(17) Patterson, G. E.; Guymon, A. J.; Riter, L. S.; Everly, M.; Griep-Raming, J.; Laughlin, B. C.; Zheng, O. Y.; Cooks, R. G. *Anal. Chem.* **2002**, *74*, 6145−6153.
(18) Tanyanyiwa, J.; Hauser, P. C. *Electrophoresis* **2004**, *25*, 3010−3016.
(19) Beard, N. P.; Edel, J. B.; deMello, A. J. *Electrophoresis* **2004**, *25*, 2363−2373.
(20) Pfeiffer, A. J.; Mukherjee, T.; Hauan, S. *Ind. Eng. Chem. Res.* **2004**, *43*, 3539−3553.
(21) Effenhauser, C. S.; Paulus, A.; Manz, A.; Widmer, H. M. *Anal. Chem.* **1994**, *66*, 2949−2953.
(22) Liu, S. R.; Shi, Y. N.; Ja, W. W.; Mathies, R. A. *Anal. Chem.* **1999**, *71*, 566−573.

10.1021/ac051014w CCC: $30.25
Published on Web 09/02/2005

migration of heterogeneous mixtures of carrier ampholytes in an electric field or through interdiffusion of reservoirs of acidic and alkalinic buffers.[23] The major difficulty in miniaturization of isoelectric focusing is to decrease the physical size of the pH gradient while still maintaining control over a wide range of pH values.

The most popular method for creating microscale pH gradients has involved exploiting microfluidic processing, where buffers are mechanically pumped from reservoirs into channels to create gradients based upon flow/diffusion. However, these methods have not shown significant improvements over macroscale methods, with separation times involving fractions of hours[24] and length scales only on the order of centimeters.[25] Further drawbacks of microfluidic processing include high-cost instrumentation,[24] the need for mechanical movement of liquid that results in parabolic velocity profiles and band broadening,[26,27] and high electric fields, which lead to Joule heating effects[28] and the possibility of gas evolution.

An alternative method employs a two-terminal electrochemical process to create a "natural" pH gradient in a simple buffer system.[25,27] Two opposing electrodes placed within a fluid channel are used to create a pH gradient by the electrolysis of water. The pH gradient forms by diffusion of OH^- and H^+ between the anode and cathode across the channel. The ability to use electric fields on the order of a few volts rather than the kilovolts needed with fluidic methods minimizes problems associated with Joule heating and gas evolution.[25,27]

Although the two-terminal electrochemical method has some advantages over microfluidic techniques, both methods suffer from slow response times. In this paper, we describe a method for generation of a microscale pH gradient that is simple, easily implemented at the microscale, controllable, reversible, and capable of generating a fully developed pH gradient on the time scale of seconds.

The method of pH gradient generation described here is based upon exploiting a surface electric field gradient. Surface electric field gradients have been previously used for a variety of applications.[29−35] This technique develops a linear potential gradient on a surface by forcing current through a resistive electrode or by holding discrete electrode locations at different applied potentials. The resulting gradient in surface potential can be used to drive electrochemical reactions that vary as a function of location on a surface. This method has been used to create surfaces with nonuniform coverage of self-assembled monolayers,[29,32,34,35] to map the potential dependence of copper deposition on gold,[33] to create nonuniform catalyst gradients,[36] and to study peptide monolayer formation on gold.[7,31] In this report, we describe the application of a surface potential gradient to create a dynamic and controllable pH gradient. The oxidation and reduction of water on a platinum-coated indium−tin oxide (ITO) electrode is manipulated by the application of a surface electric field to locally control the proton concentration in solution and generate a pH gradient near the electrode surface. The pH gradient is readily controllable, in both magnitude and direction, by simple manipulation of the applied potential values. The size of the pH gradient can be readily modified by changing the dimensions of the electrode and contact pads to allow integration into chip-scale devices. In addition, the geometry and format of this system provide a fully developed pH gradient on the time scale of seconds, as opposed to minutes or hours for competing technologies.

EXPERIMENTAL SECTION

Materials and Reagents. Metal salts ($H_2PtCl_6 \cdot 6H_2O$ and $IrCl_4$) were purchased from Aldrich (Milwaukee, WI). A pH-sensitive fluorescent probe quinine (Alfa Aesar, Lancaster, England) and universal indicator (Spectrum Chemical Mfg. Corp., Gardena, CA) were used as received. Citric acid buffers used for pH calibration were made by titrating a solution of 0.1 M citric acid monohydride, 0.1 M Na_2SO_4, ≤1 mM universal indicator, and 0.1 mM EDTA (for preservative) with 1.0 M NaOH (Aldrich) to the desired pH, using a MA130 ion meter (Meter-Toledo, Inc., Columbus, OH). When not in use, buffers were stored in a refrigerator and allowed to reach room temperature prior to use. Unless otherwise noted, solutions were prepared from as-received reagents from Fisher Scientific (Fair Lawn, NJ) in 18-MΩ deionized water (NANOPure, Barnstead, Dubuque, IA) and purged for 15 min in nitrogen before each use. Metal patterning was done with gold (Ernest F. Fullam, Inc., Latha, NY) and photoresist (Microposit S1813 Photoresist, Shipley, Marlborough, MA). Platinum−iridium wire (0.025-mm Pt90/Ir10, Goodfellow Cambridge Limited, Cambridge, England) was used for counter and pH electrodes.

Substrate Fabrication. Glass slides coated with ITO with a surface resistance of 100 Ω/in. (Delta Technologies, Stillwater, MN) were patterned with photoresist to form conducting and insulating bands of different sizes using a previously published procedure.[36] Platinum was electrodeposited onto the exposed ITO bands from a solution of ~10 mM $H_2PtCl_6 \cdot 6H_2O$ and 0.1 M Na_2SO_4 using a potentiostat (model CH1030, CH Instruments Inc., Austin, TX). A square wave potential program with limits of 0 and −1.5 V (vs Hg/Hg_2SO_4) at a frequency of 100 Hz was applied for 2 min to create a uniform layer of platinum. Contact pads to connect to the ends of the platinum-coated ITO regions were then fabricated by depositing gold through a mask that exposed the edges of the sample. Approximately 100 nm of gold was vapor-deposited (Denton Vacuum Turbo III, Morrestown, NJ) onto the ends of the substrate at a pressure of $\sim 7 \times 10^{-5}$ Torr under nitrogen atmosphere at a rate of 1−2 Å/s.

Macroscale Cell. pH gradients were initially generated and analyzed on a large sample in a macroscale electrochemical cell

(23) Righetti, P. G.; Bossi, A. *Anal. Chim. Acta* **1998**, *372*, 1−19.
(24) Hofmann, O.; Che, D. P.; Cruickshank, K. A.; Muller, U. R. *Anal. Chem.* **1999**, *71*, 678−686.
(25) Cabrera, C. R.; Finlayson, B.; Yager, P. *Anal. Chem.* **2001**, *73*, 658−666.
(26) Gottschlich, N.; Jacobson, S. C.; Culbertson, C. T.; Ramsey, J. M. *Anal. Chem.* **2001**, *73*, 2669−2674.
(27) Macounova, K.; Cabrera, C. R.; Yager, P. *Anal. Chem.* **2001**, *73*, 1627−1633.
(28) Effenhauser, C. S.; Manz, A.; Widmer, H. M. *Anal. Chem.* **1993**, *65*, 2637−2642.
(29) Terrill, R. H.; Balss, K. M.; Zhang, Y. M.; Bohn, P. W. *J. Am. Chem. Soc.* **2000**, *122*, 988−989.
(30) Wang, Q.; Bohn, P. W. *J. Phys. Chem. B* **2003**, *107*, 12578−12584.
(31) Plummer, S. T.; Wang, Q.; Bohn, P. W.; Stockton, R.; Schwartz, M. A. *Langmuir* **2003**, *19*, 7528−7536.
(32) Wang, Q.; Jakubowski, J. A.; Sweedler, J. V.; Bohn, P. W. *Anal. Chem.* **2004**, *76*, 1−8.
(33) Coleman, B. D.; Finnegan, N.; Bohn, P. W. *J. Electroanal. Chem.* **2004**, *571*, 139−148.
(34) Zhang, Y.; Terrill, R. H.; Bohn, P. W. *J. Am. Chem. Soc.* **1998**, *120*, 9969−9970.
(35) Zhang, Y. M.; Terrill, R. H.; Bohn, P. W. *Anal. Chem.* **1999**, *71*, 119−125.
(36) Jayaraman, S.; Hillier, A. C. *Langmuir* **2001**, *17*, 7857−7864.

(Figure 3A). The substrate consisted of a banded electrode with alternating Pt on ITO and insulating glass regions. The total electrode area was 12 mm × 25 mm. Gold was vapor-deposited onto the edges of the substrate to provide electrical contact to the ITO surface. The gold was connected to copper wires and secured using silver epoxy (H20E parts A and B, Epoxy Technologies, Billerica, MA) followed by an insulating epoxy (QuickSet Epoxy Gel, Hentel Consumer Adhesives, Inc., Avon, OH). Finally, the gold was insulated from the solution by Microstop stop-off lacquer (Pyramid Plastics Inc., Hope, AR). The sample was then immersed in an open-top beaker cell for analysis. Electrochemical measurements were carried out in 0.1 M Na_2SO_4 purged with N_2. The electrochemical cell used a quasi Ag/AgCl reference electrode and Pt−Ir on Ti mesh counter electrode. The counter electrode was separated from the substrate electrode by a salt bridge. The potential was controlled by a biopotenitostat (AFRDE5 Bi-potentiostat, Pine Instrument Co., Grove City, PA) with the two working electrodes connected to opposite ends of the substrate.

Microscale Flow Cell. Miniaturized pH gradients were created and analyzed in a microscale flow cell. A glass microscope slide was cut to 25 mm × 25 mm and cleaned by successive sonication in 50:50 ethanol/DI water and DI water and dried in a nitrogen stream. Double-sided adhesive tape ∼250 μm thick was placed on the slide to form a channel approximately 1000 μm wide and 2.5 cm long. An ITO-coated glass was then cut to size, patterned with platinum bands, and attached to the glass slide. The tape formed the flow channel between patterned ITO and glass pieces (Figure 4A). The exposed Pt bordered by the tape defined the electrode area. The channel was filled by capillary action and monitored with an optical microscope (Epiphot, Nikon). Electrochemical measurements were carried out in 0.1 M Na_2SO_4 purged with N_2 that also contained a universal pH indicator. Linear potential gradients were created using either the bipotentiostat or a dc power supply (PA36-3A, Kenwood Corp., Tokyo, Japan).

Fluorescence. Fluorescence measurements were performed by adding quinine to the electrolyte solution and illuminating the macrocell from the top with a 365-nm UV source (Spectroline model SB-100P, Spectronics Corp., Westbury, NY). Fluorescence was monitored with a high-resolution CCD camera (model VCC 3972, Sanyo) equipped with a variable zoom lens (Zoom 7000, Navitar), placed perpendicular to the substrate. Images were captured using commercially available software on a personal computer equipped with a frame grabber card (Pinnacle Systems, Inc., Mountain View, CA). Fluorescence intensity versus distance plots were obtained using Image J software to collect gray-scale plot profiles of the fluorescence images with respect to position within the macrochannel.

Micro-pH Electrode. pH profiles were measured in the macrocell using a miniature pH electrode. This electrode was prepared using published procedures.[37] Briefly, 250-μm-diameter platinum−iridium wire was cleaned by soaking for ∼15 min in concentrated HNO_3 (Fisher Scientific) and rinsed with water. Iridium was electrodeposited from a solution of 0.5 mM iridium(IV) chloride and 0.1 M Na_2SO_4, using a square wave potential program with limits of 0 and −1.5 V (vs Hg/Hg_2SO_4) at a frequency of 100 Hz applied for 2 min. Immediately following electrodeposition, the wire was soaked in a solution of 2 M NaOH for 20 min, followed by thermal oxidation in air at 800 °C for 1 h. The NaOH/thermal treatment was repeated three times until a uniform purple-gray coating formed on the wire. The wire was then soaked in deionized water for 3 days. The oxide coating was stripped from one end of the wire, which was then connected to a copper contact wire using silver epoxy (H20E parts A and B, Epoxy Technologies). The Pt/Ir wire was then inserted into a glass capillary (M1B000-4, World Precision Instruments, Sarasota, FL) and secured with epoxy (Quickset Epoxy Gel, Henkel Consumer Adhesives, Inc.) such that ∼5 mm of iridium oxide-coated wire protruded from one end of the capillary. Microstop stop-off lacquer (Pyramid Plastics Inc.) was used to coat the exposed sides of the wire, leaving only the end for solution contact. The open circuit potential of this electrode was then measured versus a mercury/mercury sulfate reference electrode. The voltage response of the pH electrode was calibrated against citric acid buffers using a pH meter (MA130 Ion meter, Meter-Toledo, Inc.).

pH Imaging with Universal Indicator. pH profiles in the microscale flow channel were measured using a universal pH indicator. Images of the indicator profile within the flow channel were acquired using an optical microscope and a color CCD camera (vide supra). pH profiles were then generated by taking these images and loading them into a commercial graphics software package (Canvas, Deneba). Red, orange, yellow, green, and blue hues were isolated within the images using color filters. Background images were then subtracted from the color images, and plot profiles for each of the isolated hues were obtained. An algorithm relating the five hues to the solution pH was then applied to develop the pH profiles. The algorithm consisted of a five-term linear expression relating each hue to the pH. The parameters were determined by calibration of color versus pH for a set of uniform pH standards. Notably, this procedure is limited by the nonlinearity of the CCD camera as well as optical artifacts and defects in the sample. As such, these results are limited to a precision of ±1 pH unit.

RESULTS AND DISCUSSION

The method used in this work to generate a controllable pH gradient involved applying different potential values to two spatially distinct locations on a resistive electrode surface in a manner similar to the technique originally developed by Bohn and coworkers.[34,35] By driving current between two distinct surface locations, a drop in electrode potential (ΔV) is created that follows a simple, linear relationship (eq 1),

$$\Delta V = (i\rho/A)\Delta l \tag{1}$$

where i is the electrical current, A is the cross-sectional area, ρ is the surface resistivity, and Δl is the distance along the surface. A constant surface resistivity gives a linear drop in potential between two points. When immersed in a solution, this variation in surface electrode potential can be used to drive electrochemical reactions with rates that vary along the electrode surface.[29−33]

We have exploited this method of generating a surface potential gradient to produce controllable pH gradients via oxidation and reduction reactions in water. The governing electrochemical

(37) Bordi, S.; Carla, M.; Papeschi, G.; Pinzauti, S. *Anal. Chem.* **1984**, *56*, 317−319.

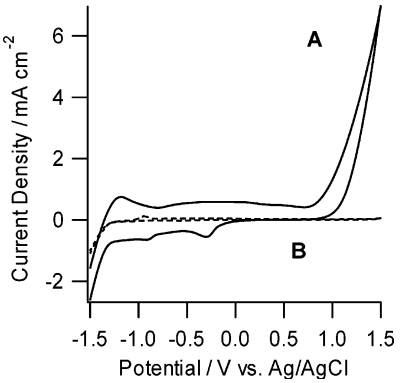

Figure 1. Cyclic voltammetry of (A) electrodeposited platinum and (B) ITO. Scan rate 0.1 V/s in 0.1 M Na_2SO_4 at pH 4.

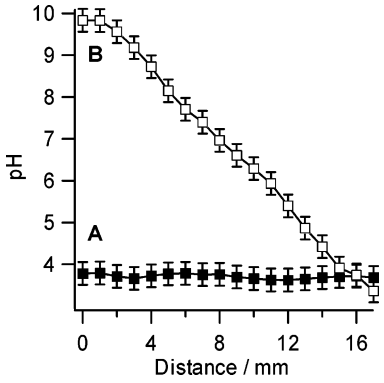

Figure 2. Measured pH profile along electrode surface determined using IrO_2 micro pH electrode. Curve A: no applied potential. Curve B: applied potential of −1 V at left and 1 V at right.

processes include pH increasing and pH decreasing reactions facilitated by a thin platinum catalyst layer. In an acidic solution, these reactions are given by

$$2H_2O \rightarrow O_2 + 4H^+ + 4e^- \qquad E^\circ\ (\mathrm{NHE}) = 1.229\ \mathrm{V} \quad (2)$$

$$2H^+ + 2e^- \rightarrow H_2 \qquad E^\circ\ (\mathrm{NHE}) = 0.0\ \mathrm{V} \quad (3)$$

The first reaction oxidizes water to produce protons and decreases the pH near the electrode surface while the second reduces the proton concentration to increase the pH. In basic solution, the reactions become

$$2H_2O + 2e^- \rightarrow H_2 + 2OH^- \qquad E^\circ\ (\mathrm{NHE}) = -0.828\ \mathrm{V} \quad (4)$$

$$2OH^- \rightarrow O_2 + 2H^+ + 2e^- \qquad E^\circ\ (\mathrm{NHE}) = 0.401\ \mathrm{V} \quad (5)$$

In each case, the reduction reaction increases the pH by either consuming protons or producing hydroxyls. The oxidation reaction lowers the pH by either generating protons or consuming hydroxyls. Notably, these reactions are also accompanied by the formation of hydrogen and oxygen gas. At sufficiently large potential values, the rate of gas evolution can exceed the solubility limit of these gases, which can lead to bubble formation on the electrode. This can be problematic in microfluidic applications. However, we have found that by carefully controlling the potential limits one can minimize or eliminate bubble formation while still influencing the local pH.

An example of reactions 2 and 3 occurring at pH 4 for both ITO and platinum surfaces is shown in the cyclic voltammetry in Figure 1. The response for Pt (Figure 1, curve A) depicts the characteristic response for this metal. The pH increases near the negative potential limit due to proton reduction (eq 2) and decreases at the positive potential limit due to water oxidation (eq 3). At intermediate potentials, the interfacial pH can be modified to a smaller extent due to the formation and removal of platinum oxides and underpotential proton adsorption. The result of these processes is an increase of solution pH near the electrode at negative potential values and a pH decrease at positive potentials. In contrast, the response of ITO (Figure 1, curve B) shows limited activity in the same potential range due to the sluggish kinetics it displays for the reactions described in eqs 2−5. The Pt layer serves to facilitate pH changes by catalyzing these pH-changing reactions.

The ability to locally control and manipulate the potential drop across the platinum-coated electrode allows precise control of the resulting pH gradient. An example pH gradient is shown in Figure 2 for a platinum-coated ITO electrode with 17-mm length. The pH profile was quantified with a custom micro-pH electrode that was scanned across the surface using a micropositioning system at a separation distance of ~100 μm. In the absence of the applied potential gradient, there is a uniform pH across the electrode surface, with a value slightly less than 4 (Figure 2, curve A), which is the same as that of bulk solution pH. A potential gradient was then applied, with the potential at the left held at $E_1 = -1$ V and the potential at the right held at $E_2 = +1$ V. In the presence of this electric field, a pH gradient develops near the electrode surface, with pH values ranging from approximately pH 10 at 0 mm to pH 3 at 17 mm. The gradient is consistent with the pH-changing reactions in eqs 2−5, where a high pH is observed at negative applied potentials and a low pH is seen at positive potentials. In addition to the variation in surface reaction rate, diffusion of ions within the liquid near the electrode surface plays a role in the shape of the pH profile.

Manipulation of the pH gradient can be readily achieved by switching of the applied potential values to influence the local rate of reaction on the electrode. Figure 3 depicts a series of images of a Pt/ITO band electrode (Figure 3A) where various pH gradients are generated. Visualization of the pH profile is achieved with the pH-sensitive fluorescence indicator quinine,[38] which fluoresces in its acidic form at pH values below its pK_a (~4.9) but remains dark in its basic form at higher pH values.

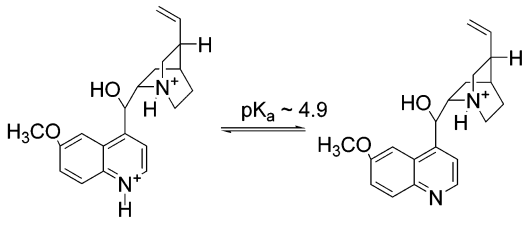

(6)

For example, Figure 3B depicts a pH gradient generated with an applied potential of $E_1 = 1$ V and $E_2 = 0.2$ V. The resulting pH

(38) Reddington, E.; Sapienza, A.; Gurau, B.; Viswanathan, R.; Sarangapani, S.; Smotkin, E. S.; Mallouk, T. E. *Science* **1998**, *280*, 1735−1737.

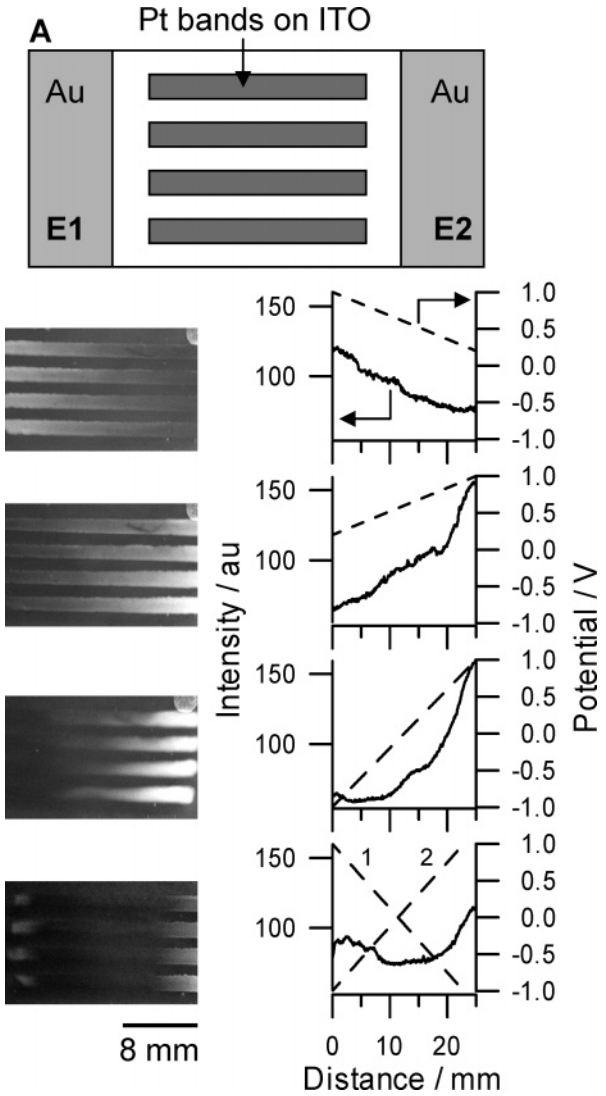

Figure 3. Examples of spatially controllable pH gradients in macrocell as visualized by fluorescence imaging. (A) Schematic of macroscale sample. Platinum bands approximately 1 mm × 25 mm are placed on an ITO substrate with gold contact pads. (B−E) Fluorescence images (left) and line plots versus distance (right) across the channel under various applied potentials in a solution of 0.1 M Na_2SO_4 with initial pH of 4. The line plots (right) depict both the fluorescence intensity (solid line) and applied potential (dashed line): (B) 1−0.2 V at E_1 and E_2, corresponding to a pH gradient of 2−6. (C) 0.2−1 V (pH gradient 6−2). (D) −1 to 1 V (pH gradient 10−2). (E) Rapid manual field switching from 1 and −1 V to −1 and 1 V applied to E_1 and E_2. The applied potential in (E) represents a combination of the two potential profiles denoted 1 and 2 in the line plot.

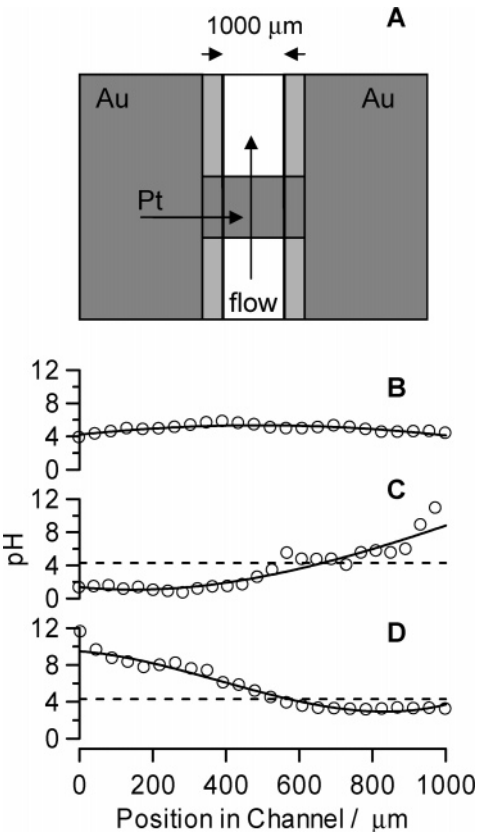

Figure 4. (A) Schematic of microscale flow cell containing gold contact pads, platinum catalyst region, and flow channel. (B−D) pH profile measured with universal indicator across the microchannel under various applied potentials. (B) No applied potential ($\Delta E = 0$ V). (C) $\Delta E = 1.86$ V. (D) $\Delta E = -2.35$ V. The dashed line in (C) and (D) represents the initial pH within the channel, and the solid lines represent a polynomial fit of the data to guide the eye.

gradient varies from a low of 2 at the left to a high of 6 at the right. As depicted in the line plot, the fluorescence intensity is high near 1.0 V on the left side of the sample, indicating an acidic pH. In contrast, the fluorescence intensity is low at 0.2 V on the right side of the sample, consistent with a slightly basic pH. Gradient reversal can be readily visualized by reversing the applied potential to $E_1 = 0.2$ V and $E_2 = 1$ V (Figure 3C). The corresponding pH gradient is reversed and now spans from pH 6 at the left to pH 2 at the right. Additional manipulation of the pH range is shown in Figure 3D, where the absolute difference between E_1 and E_2 is increased by setting $E_1 = -1$ V and $E_2 = 1$ V. This results in an increase in observed fluorescence profile, corresponding to a pH gradient with an increased width from 4 pH units to almost 8 pH units, spanning from pH 10 to pH ~2. More complex gradients can also be created. For example, Figure 3E depicts the result of dynamic switching of applied potentials. A rapid manual switching of the applied potential is performed between $E_1 = -1$ V and $E_2 = 1$ V (curve 1) to $E_1 = 1$ V and $E_2 = -1$ V (curve 2). This results in a parabolic pH profile where the edges are at a low pH while the center is at a higher pH.

The results from Figure 3 illustrate that this surface potential-generated pH gradient is easily controllable in both position and magnitude. This method enables pH gradients to be manipulated to encompass a large range of desirable pH values and physically moved along a surface. We next attempted to reduce the scale of this system to allow generation of microscale pH gradients for potential application in miniaturized analytical devices such as isoelectric focusing.

To demonstrate the ability to form a miniaturized pH gradient, we devised a microscale cell that consists of a single fluid channel of 1000-μm width, 15-mm length, and 250-μm depth, with entry/exit ports and a defined flow path (Figure 4A). Two gold contact pads were used to make electrical contact to a 3-mm-wide swath of ITO that was coated with a thin layer of Pt. The 1000-μm width for the flow channel was created by masking with a 250-μm-thick tape. The potential gradient was generated by forcing current

through the ITO layer between the two gold contact pads. Observation of pH changes was achieved using a universal pH indicator, which consisted of a mixture of pH-sensitive chromatic dyes with a detectable pH range of 3−10.

The response of the universal indicator within the microchannel cell with various electric fields is shown in Figure 4B−D. These data were produced by acquiring color images of the pH indicator, isolating various hues in the form of intensity with respect to channel position, and then converting them to pH values using a conversion algorithm. In the absence of an applied electric field, the pH across the electrode surface remains equal to that of the bulk at ~ 4 (Figure 4B). The application of a positive electric field with $\Delta E = E_1 - E_2 = +1.86$ V (Figure 4C) generates an increasing pH gradient with a low pH on the left (pH ~3) and high pH on the right (pH ≥9). This gradient is due to oxidation occurring near the left region of the electrode and reduction occurring at the right. By reversing the applied potential ($\Delta E = -2.35$ V), the pH profile across the channel transforms to a decreasing gradient with a high value on the left and a low value on the right (Figure 4D). The pH gradient in Figure 4D is approximately the same magnitude as in Figure 4C, but in the opposite direction (pH 9 to 3). As with the macroscale pH gradient demonstrated earlier with quinine, the micro pH gradient is controllable in both position and direction. However, this gradient is produced on a length scale that is considerably smaller.

In addition to the reduced length scale, the pH gradient produced with a surface electric field can respond on a much smaller time scale than competing technologies. As a comparison, two microscale flow channels of the same size were fabricated, one as described above, with a platinum layer spanning the channel and two gold contact pads. A second channel was fabricated that possessed two-terminal electrodes on a glass slide, with no connecting platinum on ITO layer. This latter configuration is reminiscent of the "natural" pH gradient method.[25,27] The channels were filled with the same solution, and an identical potential drop was applied across each channel ($\Delta E = 1.12$ V). The pH response was monitored with the universal indicator. Just before the potential was applied, both the gradient (Figure 5A) and two-terminal (Figure 5D) configurations showed a nearly constant pH value of ~4, consistent with the bulk solution. After 15 s, the gradient system showed the formation of a substantial pH profile (Figure 5B) while the two-terminal system exhibited no measurable change (Figure 5E). For the gradient sample, a pH variation ranging from a low of 3 at the left to a high of 9 at the right appeared after just 15 s while the two-terminal showed no deviation from bulk pH at this time. Only after 5 min, the two-terminal electrode system exhibited a developed pH profile of a magnitude similar to the gradient surface (Figure 5F). The gradient pH profile remained stable over this time period (Figure 5C). After 20 min, both pH profiles were stable and exhibited a comparable magnitude.

The time difference required to develop a pH gradient using the surface potential gradient versus the two-terminal "natural" gradient was compared theoretically in order to understand the origins for these differences. The local change in concentration within the microchannel was modeled by Fick's second law,

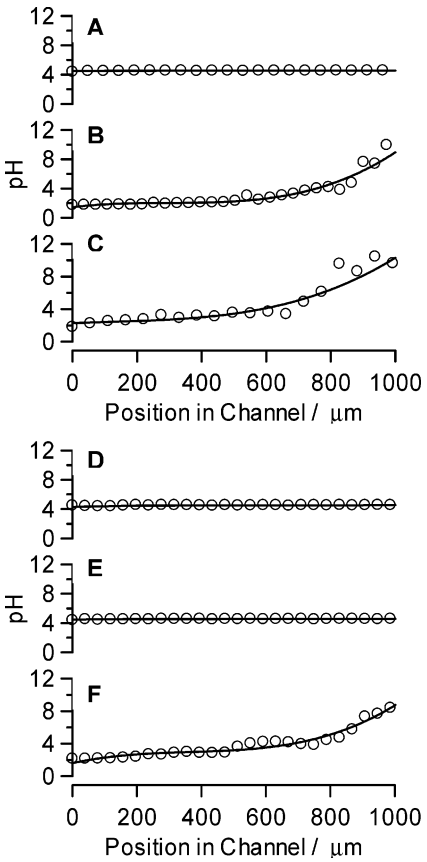

Figure 5. pH profiles within microchannel as measured with universal indicator for (A−C) potential gradient and (D−F) two-terminal electrode configuration. The data reflects pH profiles at 0 (A, C) and 15 s (B, E) and 5 min (C, F) after a potential difference of $\Delta E = 1.12$ V is applied to the edges of each sample. The solid lines represent a polynomial fit of the data to guide the eye.

using the following differential equation:

$$\frac{\partial C}{\partial t} = D\left(\frac{\partial^2 C}{\partial x^2} + \frac{\partial^2 C}{\partial y^2}\right) \tag{7}$$

where C is proton concentration, t is time, D is the proton diffusion coefficient (9.31×10^{-5} cm^2 s^{-1}), and x and y are spatial dimensions (width and height) within the channel.

Both channels were simulated with a width of 1000 μm. Boundary conditions for the pH-changing reactions were defined by the Butler−Volmer equation

$$i = -i_{o,c}e^{-(nF/RT)(E-E_{o,c})} + i_{o,a}e^{nF/RT(E-E_{o,a})} \tag{8}$$

where the exchange currents for cathodic and anodic reactions ($i_{o,c}$ and $i_{o,a}$) and the formal potentials ($E_{o,c}$, and $E_{o,a}$) were fit to experimental data for platinum in water (Figure 1A). With this information for the electrochemical current, the potential applied to the terminal electrodes or present along the surface potential gradient would dictate the local rate of electrochemical reaction. Both channels assumed potential values of −1.5 V at $x = 0$ and +1.5 V at $x = 1000$ μm for comparison. For the sample possessing a surface potential gradient, a linear potential profile is applied to the lower boundary between these two limits. The remaining

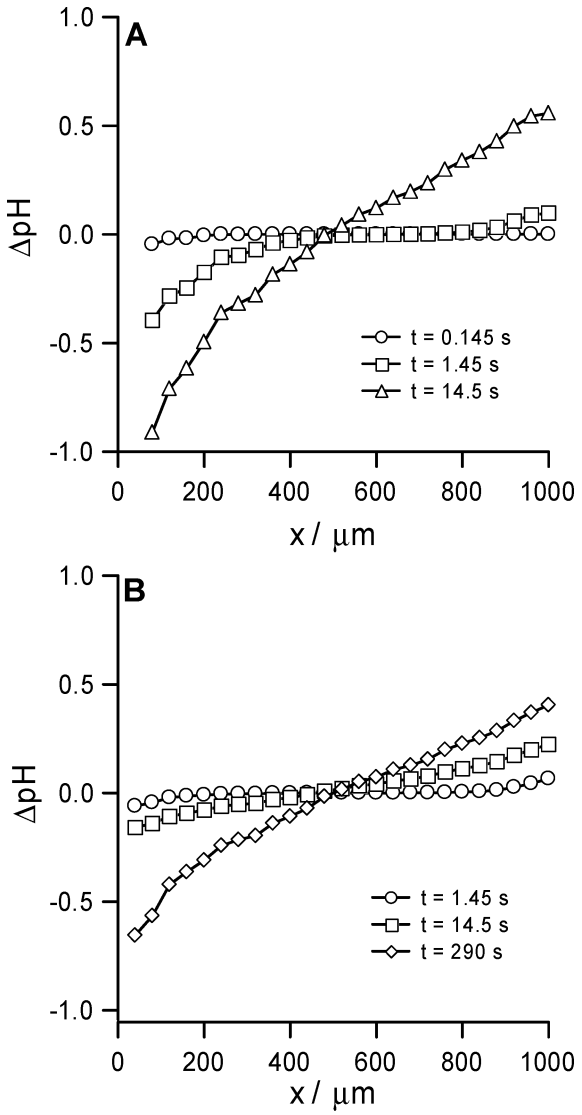

Figure 6. Simulated changes in pH within a microchannel cell for (A) potential gradient and (B) two-terminal electrode configuration at various times. The change in pH is with respect to an arbitrary initial value. Details of the simulation are provided in the text.

boundaries are treated as insulating. Finite element analysis was used to simulate the proton concentration within the channels for the two configurations. Results for the average proton concentration for each of the two configurations are plotted in Figure 6 in terms of the change in pH (ΔpH). Figure 6A shows the time evolution at $t = 0.145$, 1.45, and 14.5 s for a surface potential gradient. After only a short time, the pH has started to change within the channel having a surface potential gradient. At ~1.5 s, the pH at the left side of the channel has dropped by almost half a pH unit. At ~15 s, the pH has changed by nearly a full pH unit on each side of the channel. Although this change is not as large as was seen experimentally, the trend is similar. For comparison with the natural gradient, Figure 6B shows that the evolution of pH in the two-terminal configuration is much slower. At ~1.5 s, the pH has changed only slightly at the edges of the channel. Further changes in the pH have occurred by ~15 s, but not near the magnitude of that seen in the gradient system. To achieve a pH change of a magnitude similar to that seen for the potential gradient at 15 s, the two-terminal system requires 290 s or ~5 min. This difference in time scale is a factor of almost 20.

The substantially decreased time scale required to develop a pH gradient using an electrode with a surface potential as compared to the two-terminal system can be rationalized by considering the role of diffusion. In the two-terminal system, a fully established pH profile requires that protons or hydroxyls diffuse across the channel width. In contrast, the potential gradient involves a much smaller diffusion path. Since the reaction is occurring along the surface of the channel, we can assume that protons and hydroxyls are produced instantaneously at the channel floor and then need only to diffuse the height of the channel. Since the time required for diffusion is proportional to the square of the distance involved, diffusion across the 1000-μm channel width takes 25 times longer than diffusion up the 200-μm channel height. This difference is nearly identical to the experimentally observed and theoretically predicted variation between the two systems.

CONCLUSIONS

This report describes a method for the rapid and reversible generation of a microscale pH gradient using a spatially varied, surface electric field. Benefits of using this method to produce a pH gradient include the ability to readily control both the position and magnitude of the pH gradient. In addition, this method is scalable, allowing the formation of gradients ranging from centimeters in size down to micrometers, depending upon the length over which the electric field is applied. The time response of this method when working in a thin channel or microscale platform is considerably improved over competing technologies. Indeed, the ability to modulate the pH within a microscale channel within mere seconds is a substantial advance for chip-scale separation devices. It is anticipated that this work will impact on a variety of chip-scale analytical devices, protein separation techniques, and combinatorial pH studies. Indeed the ability to create a variable pH profile might have further application in the study of corrosion processes, metal deposition, enzyme reactions, metabolic processes, or any other chemical system involving pH as a variable.

ACKNOWLEDGMENT

The authors gratefully acknowledge the National Science Foundation (CTS 0405442) and Iowa State University for partial support of this work.

Received for review June 8, 2005. Accepted August 3, 2005.

AC051014W